

Near-Field Imaging of a Silver Nanowire Using a Thin Silver Film

Zhengtong Liu, Alexander V. Kildishev*, Vladimir P. Drachev, and Vladimir M. Shalaev

Birck Nanotechnology Center, Department of Electrical and Computer Engineering
Purdue University, West Lafayette, IN 47907, USA
kildishev@purdue.edu

Abstract: This work deals with the near-field, sub-wavelength imaging of nanoscale objects using a thin silver film (near-field lens, NFL). As an example object, we consider a thin circular nanowire illuminated by a p -polarized plane wave. The simulation considers the coupling between the object and the lens and is based on the addition theorems of cylindrical and plane waves. We compare the realistic imaging regime with object-image coupling versus an artificial regime with no coupling effect. In addition, the localized field enhancement transfer is also investigated with realistic loss in the film. The simulation results show that a shadow image of the wire can be obtained at the imaging plane. The results also demonstrate that the field enhancement resulting from the localized surface plasmon resonance at the wire surface can be transferred to the other side of the lens. The coupling between the wire and the lens acts to decrease the overall enhancement transferred to the imaging side of the lens.

Keywords: near-field imaging, near-field lens, thin silver film, superlens

1. Introduction

Negative index metamaterials (NIMs) have attracted extensive attention recently [1]. One of the applications of NIMs is sub-wavelength near-field imaging (NFI), which uses a thin slab of NIM as a superlens. The general requirements for NIM functionality are $\text{Re}(\epsilon) < 0$ for permittivity and $\text{Re}(\mu) < 0$ for permeability. Recently it was pointed out by Pendry [2] that in the electrostatic limit and for imaging with a p -polarized wave, only negative permittivity, $\text{Re}(\epsilon) < 0$, would be sufficient for NIM functionality. Some metals (e.g., silver, gold, and copper) have the required permittivity, and simulation results have shown that sub-wavelength imaging can indeed be theoretically achieved by a superlens made of these metals [3]-[6]. Subsequent experimental results have confirmed the sub-wavelength imaging capability of metallic film lenses [7], [8].

In most of the reported simulations, however, the objects imaged are hypothetical slits and are rather different from the metal masks used in experiments, since mask-superlens coupling may play an important role in the overall result. The role of the mask-superlens coupling has not yet been analyzed in detail. Another issue is that typically only the magnetic field is studied in the literature. Although in the far field the electric field is proportional to magnetic field, the fields can have different distributions in the near-field zone. In this paper, we use a circular cylindrical wire as a realistic imaging object, and analyze both the electric and magnetic fields in the near-field zone.

The classical scattering problem of a cylinder in front of a plane interface has been studied by many researchers [9]-[13]. Borghi *et al.* have used an expansion of cylindrical waves to obtain an analytical solution [9], [10], and Valle *et al.* used the extinction theorem to calculate the field [11]-[13] for such a system. In this paper, we use the cylindrical wave approach to study the near-field regime. Our interests are not limited to the imaging properties of the silver lens; we are also interested in the field enhancement after the lens, since the coupled system has exciting potential applications in techniques such as surface-enhanced Raman scattering (SERS).

2. Mathematical formulation

The geometry of the wire-lens system is shown in Fig. 1. The NFL is a thin silver film of thickness d . An infinitely long, thin wire (a circular cylinder) is placed in front of the lens with its axis parallel to the lens interface. The radius of the wire is a and the center-to-interface distance is b . The NFL and the object are illuminated by a p -polarized plane wave with $\vec{H}_0 = \hat{z}h_0$ (where $h_0 = e^{ikx}$) and $\vec{E} = \hat{y}(i\omega\varepsilon)^{-1}h_0'$, where $h_0' = \partial_x h_0$ and ε is the complex permittivity of silver.

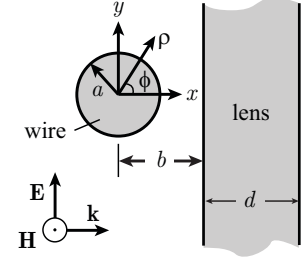


Fig. 1. Wire-lens geometry.

Our method is similar to that used in Refs. [9] and [10]. For normal incidence, we have the following equations for the magnetic fields in front of the lens:

$$h_i = \sum_{m=0}^{\infty} c_i^m C_i^m, \quad \rho \leq a; \quad h_s = \sum_{m=0}^{\infty} c_s^m C_s^m, \quad \rho \geq a, \quad (1)$$

where h_i is the summation of all fields traveling towards the cylinder, h_s is the scattered magnetic field, k is the wavevector in free space, $C_i^m = J_m(k\rho)\cos m\phi$, $C_s^m = H_m^{(1)}(k\rho)\cos m\phi$, and J_m , $H_m^{(1)}$ are the Bessel and Hankel functions. The spatial spectral coefficients c_s^m are related to c_i^m by $c_s^m = s^m c_i^m$, where s^m is determined by the refractive index of the nanowire n and its radius a through the following ratio [14]: $s^m = -(nJ_m(nka)\partial_a J_m(ka) - J_m(ka)\partial_a J_m(nka)) / (nJ_m(nka)\partial_a H_m^{(1)}(ka) - H_m^{(1)}(ka)\partial_a J_m(nka))$.

After truncating the series in (1) at $m = m_{\max}$, we can rewrite $c_s^m = s^m c_i^m$ in a matrix form,

$$\mathbf{c}_s = \mathbf{s}\mathbf{c}_i, \quad (2)$$

where \mathbf{c}_i and \mathbf{c}_s are column vectors $\mathbf{c}_i = [c_i^m]$ and $\mathbf{c}_s = [c_s^m]$, and \mathbf{s} is a diagonal matrix, $[s]_{mm} = s^m$.

The incident wave is a p -polarized plane wave, and its magnetic field h_0 is approximated by the product $h_0 = \mathbf{j}^T \mathbf{c}_0$, where \mathbf{j} and \mathbf{c}_0 are column vectors, $\mathbf{j} = [C_i^m]$ and $\mathbf{c}_0 = [c_0^m]$. Note that $c_0^m = 2i^m$, if $m > 0$, and $c_0^0 = 1$. The incident field h_0 and the scattered field h_s are reflected by the lens, giving the fields h_{0r} and h_{sr} . The reflected plane wave h_{0r} can be straightforwardly expressed as $h_{0r} = r_0 e^{2ikb} \mathbf{j}^T \mathbf{c}_{0r}$, where r_0 is the reflection coefficient at normal incidence, and $c_{0r}^l = 2i^{-l}$, $l > 0$, and $c_{0r}^0 = 1$. Taking the Fourier transform of h_s at the metal-air interface with respect to the wave vector along the y direction and taking reflection into account, we then obtain h_{sr} as

$$h_{sr} = \mathbf{j}^T \mathbf{q} \mathbf{c}_s, \quad (3)$$

where \mathbf{q} is the interaction matrix showing that a single mode cylindrical wave is redistributed into other modes after reflection. Square matrix \mathbf{q} is defined as $\mathbf{q} = [q_{lm}]$, where each element q_{lm} is given by an integral transformation $q_{lm} = \pi^{-1} \int_0^\infty r(\alpha) f_m(\alpha) g_l(\alpha) e^{2ik\beta b} d\alpha$. $r(\alpha)$ is the plane wave mode reflection coefficient; f_m and g_l are the transfer functions given by $f_m(\alpha) = [(\alpha - i\beta)^m + (-1)^m (\alpha + i\beta)^m] \beta^{-1}$ and $g_l(\alpha) = (\alpha - i\beta)^l + (-1)^l (\alpha + i\beta)^l$ for $l \neq 0$, and $g_0(\alpha) = 1$; the normalized wave vectors along x and y directions, α and β , are connected by $\beta = \sqrt{1 - \alpha^2}$.

Eq. (3) defines the matrix form of the addition theorem connecting the reflected cylindrical wave expansions. The fields h_0 , h_{0r} , and h_{sr} act together as a set of cylindrical waves coming towards the wire;

therefore, $h_i = h_0 + h_{0r} + h_{sr} = \mathbf{j}^T \mathbf{c}_i$ and

$$\mathbf{c}_i = \mathbf{c}_0 + r_0 e^{2ikb} \mathbf{c}_{0r} + \mathbf{q} \mathbf{c}_s. \tag{4}$$

Combining (2) and (4), we find the solution for \mathbf{c}_s :

$$\mathbf{c}_s = (\mathbf{i} - \mathbf{s} \mathbf{q})^{-1} \mathbf{s} [\mathbf{c}_0 + r_0 e^{2ikb} \mathbf{c}_{0r}]. \tag{5}$$

The coefficients \mathbf{c}_s give the solution for the distribution of both the magnetic and electric fields in the wire-lens system.

In a similar manner, the transmitted magnetic field after the lens is given by $h_t = t_0 e^{ik(b+x)} + \mathbf{p}_t \mathbf{c}_s$, where \mathbf{p}_t is a row vector with $p_t^m = \frac{1}{2\pi} \int_{-\infty}^{\infty} t(\alpha) f_m(\alpha) e^{ik\beta b} e^{ik(\beta x + \alpha y)} d\alpha$, and $t(\alpha)$ is the plane wave transmission coefficient of the lens¹. Then, in any region with a given distribution of the total magnetic field h and complex permittivity ϵ , the electric field \vec{E} is calculated using one of Maxwell's equations, $\vec{E} = (\omega\epsilon)^{-1} \hat{\mathbf{z}} \times \nabla h$. We note that removing the products $\mathbf{s} \mathbf{q}$ and $r_0 e^{2ikb} \mathbf{c}_{0r}$ from (5) results in a ‘‘no coupling’’ situation and no adjustments are required for the field expansions inside and beyond the lens. Thus, in addition to adequate accuracy, the available option of ‘‘switching off’’ the feedback interaction between the object and the lens is an important feature of our simulation approach.

3. Results and discussion

We have simulated the geometry given by $a = 25$ nm, $b = 35$ nm, and $d = 20$ nm at a wavelength of 340 nm. The refractive index of silver is taken from Ref. [15]. The permittivity of silver at 340 nm is

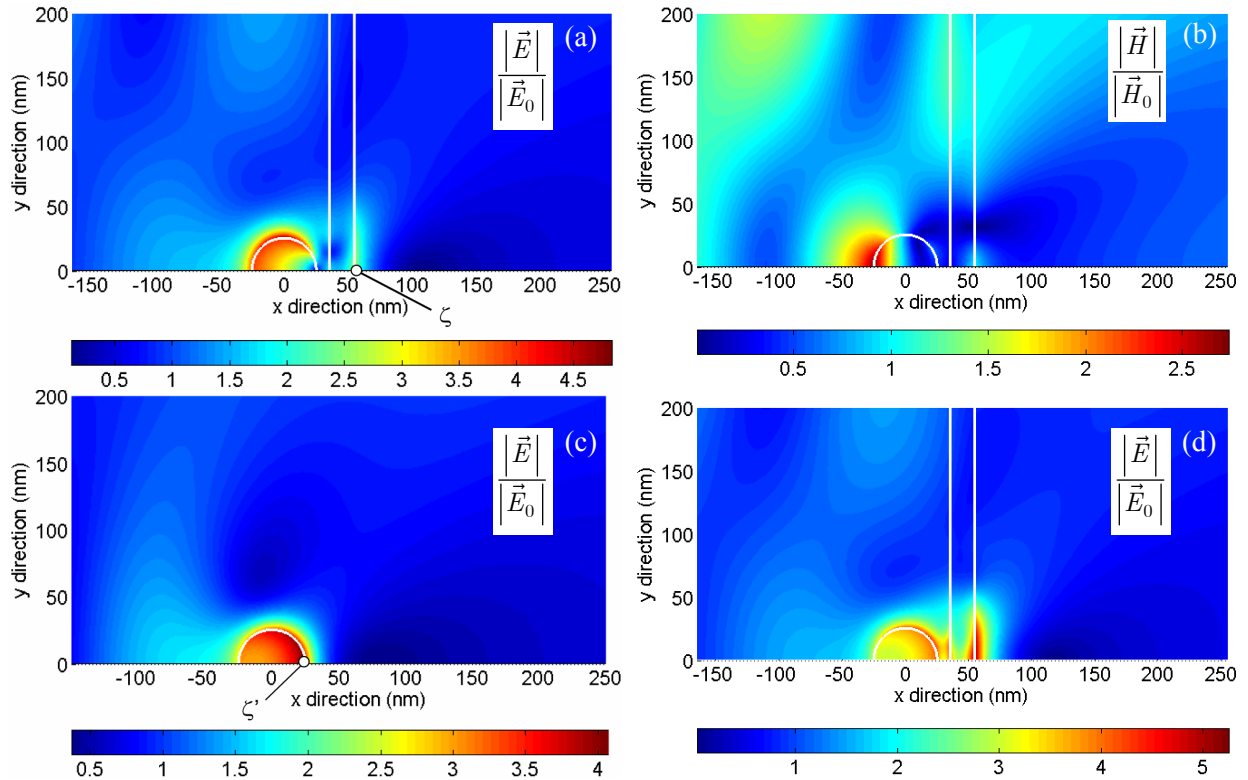


Fig. 2. (a) The normalized electric field and (b) the normalized magnetic field of the wire-lens system. (c) The normalized electric field of a single cylinder. (d) The normalized electric field of the wire-lens system without coupling. (Only half of each field map is shown due to symmetry.)

$-1.17 + 0.28i$, which is close to the surface plasmon resonance condition. The electric and magnetic fields are plotted in Fig. 2 (a) and (b) respectively, and they are clearly distinct. After the lens there is a shadow region where the electric field is low, which is considered to be the near-field shadow of the cylinder. In comparison, the magnetic field in Fig. 2(b) does not exhibit this shadow feature. As shown in Fig. 2(c), a similar shadow (negative image) is present without the lens, and the lens clearly translates the image in the x direction.

Fig. 2(a) also shows that the incident electric field can be increased beyond the lens with an enhancement factor of about two (at point ζ). For comparison, the electric field of the same wire without the lens is shown in Fig. 2 (c). In this case, the best enhancement factor is about four at ζ' (a location close to the cylinder surface). This result demonstrates the possibility of transferring the field enhancement from the nanowire surface to the other side of the lens, albeit with a loss. The spectral behavior of the normalized fields at point ζ is plotted in Fig. 3. The highest electric field enhancement (about 2.7) occurs at a wavelength of 340 nm. This wavelength is coincident with the surface plasmon resonance wavelength and is where the superlens effect is predicted [2].

We have also simulated the wire-lens system without coupling. This is a hypothetical situation where the reflected wave h_{or} and h_{sr} are not scattered by the wire. Therefore, there is no feedback interaction between the reflected and scattered fields of the lens and the wire. The result in this situation is shown in Fig. 2(d). A comparison of Figs. 2(a) and (d) clearly indicates that the coupling between the wire and the lens plays an important role, modifying the field distribution and suppressing the electric field enhancement beyond the lens.

For example, Fig. 4(a) shows the near-field modes ($\alpha_1 = 4.25$ and $\alpha_2 = 5$) transmitted through the silver lens. For $\alpha_1 = 4.25$, the electric field without the lens almost overlaps with the electric field with the lens after a displacement of about $2d = 40$ nm. For larger values of α the optimal displacement is smaller, but still close to 40 nm. This result is further illustrated in Fig. 4(b), where two sets of contours of the electric fields behind the wire with and without the lens are plotted. The sets of contours are almost identical aside from a constant scaling factor, which is due to losses in the silver film. The lens translates the shadow image with a displacement of 37 nm, which is close to the source-image distance of $2d$ shown in Ref. [2].

In summary, we have studied the imaging of a realistic object (a silver nanowire), in contrast to the conventional imaging analysis of hypothetical slits. The object was illuminated by a p -polarized plane wave. Without the lens the object produces a near-field shadow (negative image) where the field intensity is lower than the back-

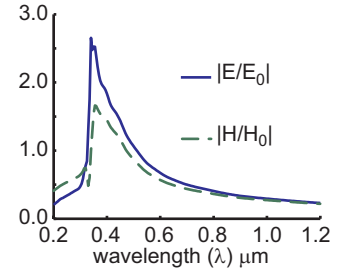


Fig. 3. The normalized fields at the lens interface.

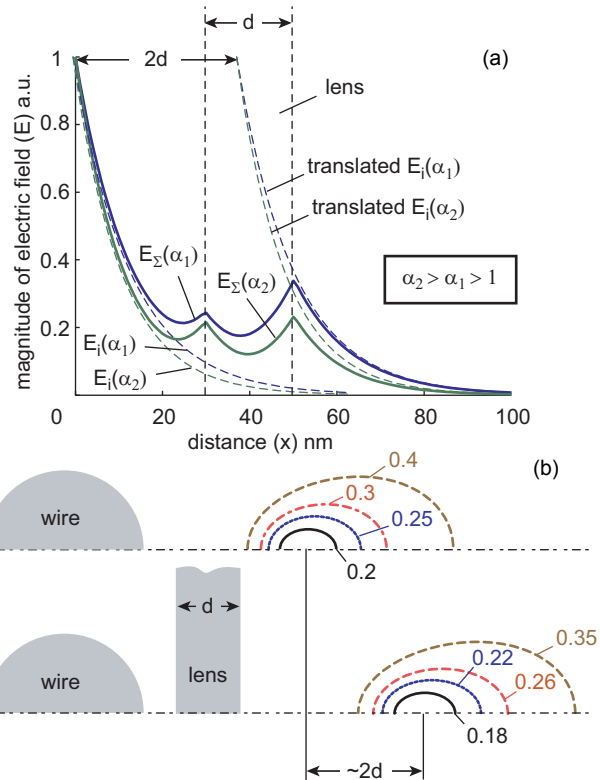


Fig. 4. (a) Simulated transformation of the E-field magnitude of different near-field modes. $E_i(\alpha_1)$ and $E_i(\alpha_2)$ are non-propagating components of a near-field source, where $E_s(\alpha_1)$ and $E_s(\alpha_2)$ are the magnitudes of the total E-field. (b) The contours of normalized electric fields both with and without the lens. The shadow image is shifted by 37 nm by the 20-nm-thick lens.

ground. (This is not surprising since a slit allows light to pass through, while a cylinder blocks light.) It is also shown that a thin silver film translates the negative image of the object to the imaging plane. The lens is also capable of transferring the field enhancement resulting from the surface plasmon resonance of the silver nanowire to the image side of the lens. The coupling between the wire and the lens decreases the transferred enhancement.

4. Acknowledgments

This work was supported in part by ARO grant W911NF-04-1-0350, NSF-PREM Grant #DMR-0611430 and by ARO-MURI award 50342-PH-MUR.

References

- [1] A. V. Kildishev, W. Cai, U. K. Chettiar, H.-K. Yuan, A. K. Sarychev, V. P. Drachev, and V. M. Shalaev, "Negative refractive index in optics of metal-dielectric composites", *J. Opt. Soc. Am. B*, Vol. 23, pp. 423-433, 2006
- [2] J. B. Pendry, "Negative refraction makes perfect lens", *Phys. Rev. Lett.*, Vol. 85, pp. 3966-3969, 2000.
- [3] S. A. Ramakrishna, J. B. Pendry, D. Schurig, D. R. Smith, and S. Schultz, "The asymmetric lossy near-perfect lens", *J. Mod. Optic.*, Vol. 49, pp. 1747-1762, 2002.
- [4] S. A. Ramakrishna, J. B. Pendry, M. C. K. Wiltshire, and W. J. Stewart, "Imaging the near field", *J. Mod. Optic.*, Vol. 50, pp. 1419 - 1430, 2003.
- [5] S. Jiang and R. Pike, "A full electromagnetic simulation study of near-field imaging using silver films", *New J. Phys.*, Vol. 7, Article No. 169, 2005.
- [6] S. Feng and J. M. Elson, "Diffraction-suppressed high-resolution imaging through metallodielectric nanofilms", *Opt. Express*, Vol. 14, pp. 216-221, 2006.
- [7] N. Fang, H. Lee, C. Sun, and X. Zhang, "Sub-diffraction-limited optical imaging with a silver superlens", *Science*, Vol. 308, pp. 534-537, 2005.
- [8] H. Lee, Y. Xiong, N. Fang, W. Srituravanich, S. Durant, M. Ambati, C. Sun, and X. Zhang, "Realization of optical superlens imaging below the diffraction limit", *New J. Phys.*, Vol. 7, Article No. 255, 2005.
- [9] R. Borghi, F. Gori, M. Santarsiero, F. Frezza, and G. Schettini, "Plane-wave scattering by a perfectly conducting circular cylinder near a plane surface: cylindrical-wave approach", *J. Opt. Soc. Am. A*, Vol. 13, pp. 483-493, 1996.
- [10] R. Borghi, M. Santarsiero, F. Frezza, and G. Schettini, "Plane-wave scattering by a dielectric circular cylinder parallel to a general reflecting flat surface", *J. Opt. Soc. Am. A*, Vol. 14, pp. 1500-1504, 1996.
- [11] P. J. Valle, F. González, and F. Moreno, "Electromagnetic wave scattering from conducting cylindrical structures on flat substrates: study by means of the extinction theorem", *Appl. Optics*, Vol. 33, pp. 512-522, 1994.
- [12] P. J. Valle, F. Moreno, J. M. Saiz, and F. González, "Near-field scattering from subwavelength metallic protuberances on conducting flat substrates", *Phys. Rev. B*, Vol. 51, pp. 13681-13690, 1995.
- [13] A. Madrazo and M. Nieto-Vesperinas, "Scattering of electromagnetic waves from a cylinder in front of a conducting plane", *J. Opt. Soc. Am. A*, Vol. 12, pp. 1298-1309, 1995.
- [14] C. F. Bohren and D. R. Huffman, *Absorption and Scattering of Light by Small Particles*, John Wiley & Sons, 1983.
- [15] P. B. Johnson and R. W. Christy, "Optical constants of the noble metals", *Phys. Rev. B*, Vol. 6, pp. 4370-4379, 1972.